

# Fluorescence polarization studies of autoionization in CS<sub>2</sub>

E. D. Poliakoff

*Department of Chemistry, Boston University, Boston, Massachusetts 02215*

J. L. Dehmer

*Argonne National Laboratory, Argonne, Illinois 60439*

A. C. Parr

*National Bureau of Standards, Gaithersburg, Maryland 20899*

G. E. Leroi

*Department of Chemistry, Michigan State University, East Lansing, Michigan 48824*

(Received 17 October 1986; accepted 21 November 1986)

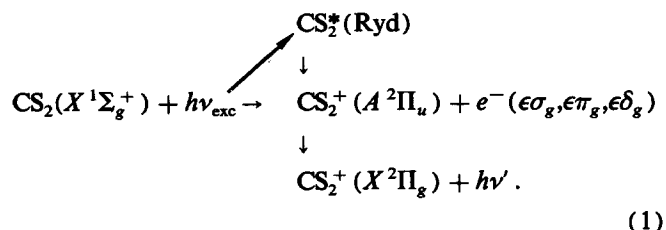
The polarization of the CS<sub>2</sub><sup>+</sup> (*A*<sup>2</sup>Π → *X*<sup>2</sup>Π) transition was measured following photoionization of CS<sub>2</sub> with synchrotron radiation excitation in the range 875 Å < λ<sub>exc</sub> < 967 Å. Autoionization features are prominent in the fluorescence polarization spectrum and were investigated in detail. The spectral assignments of the absorption spectrum by Ogawa and Chang [Can. J. Phys. 48, 2455 (1970)] are supported by the current measurements. Although fluorescence excitation and fluorescence polarization profiles normally align precisely, exceptions have been found for many resonances (σ<sub>u</sub> → *nd*π, *n* > 3), and comparisons between the line shapes are given for several features.

## I. INTRODUCTION

Molecular autoionization has been the focus of extensive theoretical and experimental efforts<sup>1</sup> aimed at understanding the dynamics of channel interaction in the electronic continua of small molecules. Molecular electronic autoionization is the process by which a Rydberg level converging to an excited electronic state of the ion exchanges electronic (and possibly vibrational and rotational) energy with the molecular core, resulting in decay into the underlying ionization continua. There are many studies that have provided insight into the process; however, the identity of the quasisdiscrete state undergoing autoionization is poorly characterized for many molecular systems, owing to the congestion of the autoionization spectra with overlapping and interacting Rydberg series. Recently, we showed<sup>2</sup> that when the ion is created in a (fluorescing) excited electronic state, fluorescence polarization can be exploited to label the electronic symmetry of the autoionizing Rydberg level. The physical basis for this is that the electronic symmetry of the autoionizing state influences the orientation of the absorption transition dipole in the molecular frame. The *m<sub>j</sub>* level distribution of the product ion, i.e., its alignment, is influenced by the symmetry of the resonantly excited Rydberg level. The resulting fluorescence polarization, in turn, depends on the molecular ion's alignment, thus serving as a beacon for the electronic symmetry of the autoionizing level. This reasoning has been used in the earlier investigation of CO<sub>2</sub> autoionization,<sup>2</sup> and in this paper, we report experiments on CS<sub>2</sub> which extend the earlier work.

CS<sub>2</sub> serves as a useful test case for several reasons. First, high quality photoabsorption spectra<sup>3-6</sup> are available, and the spectroscopic assignments are better determined<sup>3</sup> than for most molecular systems. Similarly, photoionization mass spectra are available.<sup>7-9</sup> Moreover, the autoionization features are well separated for CS<sub>2</sub> and many of the features are rather broad so that the fluorescence excitation and polar-

ization profiles can be probed sensitively using the moderate spectral resolution available for the present studies (Δλ<sub>exc</sub> ~ 0.8 Å). The comparison between fluorescence polarization and fluorescence excitation spectra is particularly important to test the simple mixing procedure employed in the earlier CO<sub>2</sub> analysis.<sup>2</sup> The excitation and fluorescence transitions investigated here are analogous to those studied in the earlier CO<sub>2</sub> work<sup>2</sup> and are described by Eq. (1):



While fluorescence polarization analysis for atomic autoionization has been characterized in some detail theoretically,<sup>10</sup> that for molecular autoionization has not, aside from the limited classical modeling used for the CO<sub>2</sub> studies. Theoretical advances have made it possible to probe electronic interchannel coupling in molecular photoionization,<sup>1,11-14</sup> so polarization data can serve as useful input for spectroscopic labeling of the Rydberg state. Furthermore, the present measurements indicate the possibility that the polarization measurements might also provide dynamical information. The utility and the limitations of such measurements are highlighted by the present results.

These measurements also provide a stepping stone to more comprehensive studies; in particular, the present results were obtained without dispersing the fluorescence. However, technical advances in synchrotron radiation facilities make it possible to extend these studies to the vibrationally resolved level.<sup>15-17</sup> In addition to their intrinsic value, the results of the current measurements provide considerable impetus for such refinements, as weaker resonance phe-

nomena may be probed selectively and sensitively using dispersed fluorescence polarization analysis.

## II. EXPERIMENTAL

The apparatus has been described previously<sup>2,18</sup> and is illustrated schematically in Fig. 1. The excitation radiation originates from the electron storage ring at the Synchrotron Ultraviolet Radiation Facility (SURF-II) at the National Bureau of Standards. The radiation is monochromatized by a 2 m normal incidence monochromator,<sup>19</sup> operated at 0.8 Å bandwidth for the present measurements. The uncertainty in the wavelength scale is estimated to be 0.4 Å and the photon flux is typically  $3 \times 10^{10}$  photons/s. A differentially pumped capillary channels the radiation to the interaction region where it intersects an effusive molecular beam. A 1000 L/s cryopump maintains the chamber pressure at  $10^{-4}$  Torr during the experiments, and we estimate the effective pressure in the interaction region to be a factor of 10 greater. The fluorescence is collected at right angles to both the propagation axis and the polarization vector of the excitation radiation. A 25 mm diameter, 25 mm focal length plano-convex lens collects the fluorescence radiation and the collimated beam exits the vacuum chamber through a suprasil window. With this collection geometry, approximately 4% of the total solid angle is directed towards the detector. The fluorescence passes through a Polaroid HNPB sheet polarizer and is detected by an RCA C31000A photomultiplier tube, cooled to  $-30$  °C. The dark count contribution is assessed by closing an electrical shutter to block out the fluorescence

during half of the data collection cycle for all data points.

Data are collected in two modes: excitation spectra and fluorescence polarization spectra. For an excitation spectrum, the total CS<sub>2</sub><sup>+</sup> fluorescence intensity is measured with the polarizer removed as a function of the excitation wavelength. A photodiode is used to monitor the VUV radiation fluence for all data points. Spectra are corrected for the incident radiation intensity, which decays with the stored electron beam. However, the excitation spectrum is *not* corrected for the wavelength response of the photodiode, which is slowly varying throughout the region studied. The polarization spectra are obtained in the same manner as has been described previously. The polarization index employed in this work is defined as  $P = (I_{\parallel} - I_{\perp}) / (I_{\parallel} + I_{\perp})$ . The fluorescence polarization results are corrected for the incomplete polarization of the excitation radiation, i.e., the values presented are those which would be obtained with completely linearly polarized excitation radiation. The data collection is controlled by a LSI 11 microcomputer interfaced to a CA-MAC crate with appropriate control and scaling modules.

## III. RESULTS

A fluorescence excitation spectrum of CS<sub>2</sub><sup>+</sup> is shown in the lower frame in Fig. 2. Previous work<sup>20,21</sup> indicates that the observed fluorescence should be predominantly from the CS<sub>2</sub><sup>+</sup> ( $A \rightarrow X$ ) transition ( $4350 \text{ \AA} < \lambda_n < 5700 \text{ \AA}$ ) in the excitation energy range studied. The fluorescence excitation spectrum agrees well with those from previous investigations.<sup>4,20</sup> There are three established Rydberg series in this region,<sup>3</sup> and they are indicated at the bottom of Fig. 2. The labeled lines are assigned as  $v = 0$  Rydberg levels and the four unlabeled features in the  $nd\sigma$  and  $ns\sigma$  series correspond

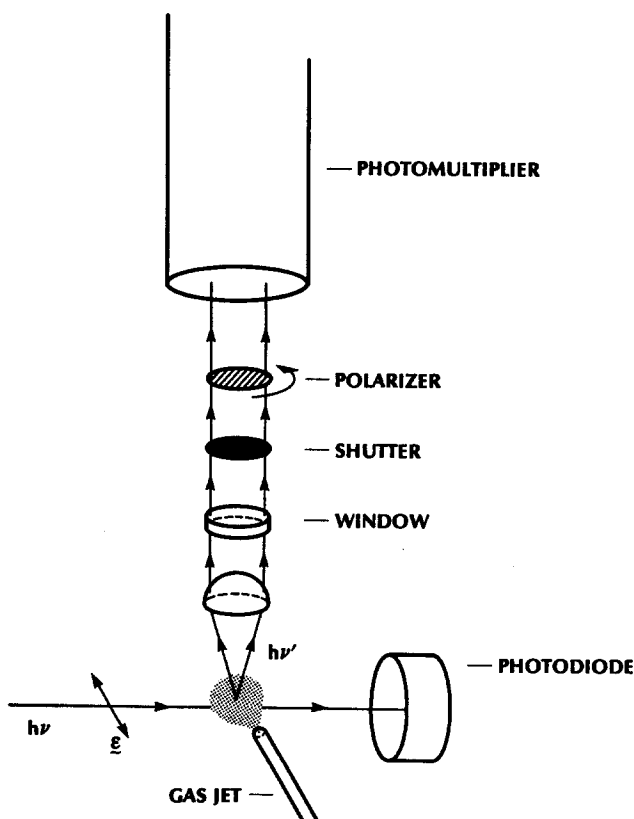


FIG. 1. Experimental schematic. The individual components and their functions are discussed in the text.

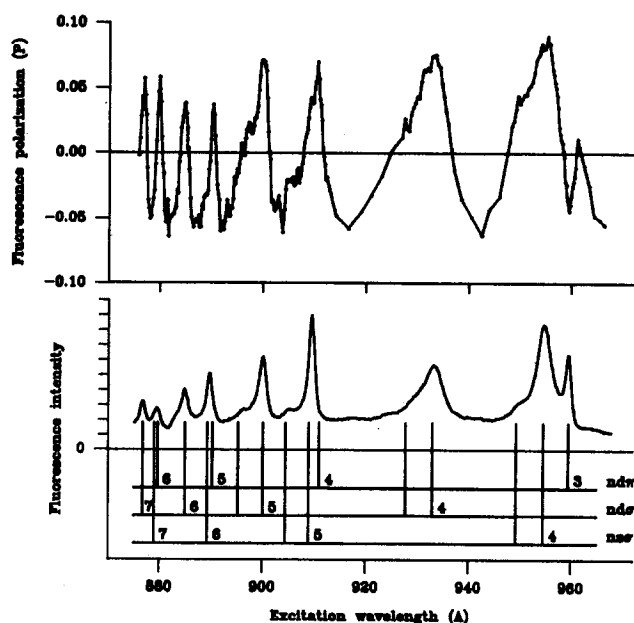


FIG. 2. Lower frame: fluorescence excitation spectrum of CS<sub>2</sub><sup>+</sup> ( $A \rightarrow X$ ) and spectral assignments from Ogawa and Chang (Ref. 3). The labeled members are assigned as  $v = 0$  members of the Rydberg series and the four unlabeled features in the  $nd\sigma$  and  $ns\sigma$  series correspond to  $v = 1$  levels. Upper frame: fluorescence polarization measurements as a function of the excitation wavelength.

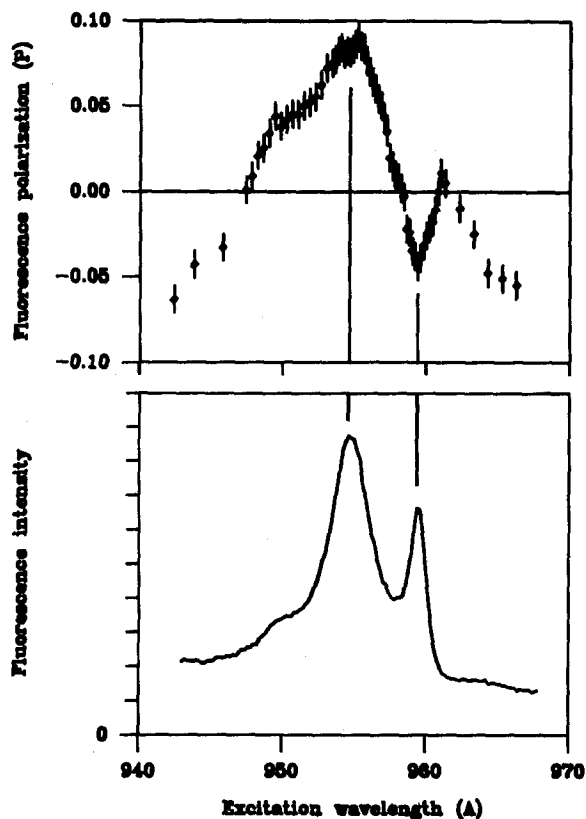


FIG. 3. Expanded view of fluorescence excitation and fluorescence polarization spectra in region of the  $3d\pi$  and  $4s\sigma$  ( $\nu_R = 0,1$ ) resonances. Note that the fluorescence polarization displays a maximum in the vicinity of the  $\sigma$  resonance and a minimum in the region of the  $\pi$  resonance.

to  $v = 1$  Rydberg levels. Except for the lowest members, the  $nd\pi$  Rydberg series is not well separated from the  $ns\sigma$  series.

The fluorescence polarization spectrum is plotted in the top frame of Fig. 2, and all of the fluorescence excitation peaks have corresponding features in the fluorescence polarization spectra. Close inspection of the excitation vs polarization behavior reveals several interesting facets. For example, Fig. 3 shows the region of the  $3d\pi$  and  $4s\sigma$  resonances, and while the  $4s\sigma$  feature exhibits a peak in the polarization spectrum, the polarization displays a minimum at the  $3d\pi$  resonance excitation wavelength. Figure 3 also shows that the maxima in the excitation spectra line up precisely with the polarization extrema.

Yet, features in the excitation and polarization spectra need not align precisely. Indeed, there are some features that exhibit shifts between the two spectra. For example, Fig. 4 shows the polarization and excitation spectra in the region of the  $5s\sigma$  and  $4d\pi$  peaks, and the polarization maximum is shifted  $0.9 \text{ \AA}$  to higher wavelength from the excitation maximum. At first, one might attribute this shift to experimental uncertainties. However, the polarization data have an internal calibration with respect to the excitation spectra because the  $I_{\parallel}$  and  $I_{\perp}$  components are determined individually (and stored separately on disk) to determine the polarization index  $P$ . Note that the denominator of the polarization index is the same as the total fluorescence observed in the fluorescence excitation measurements. So, by plotting both the denominator of the polarization fraction and the polarization

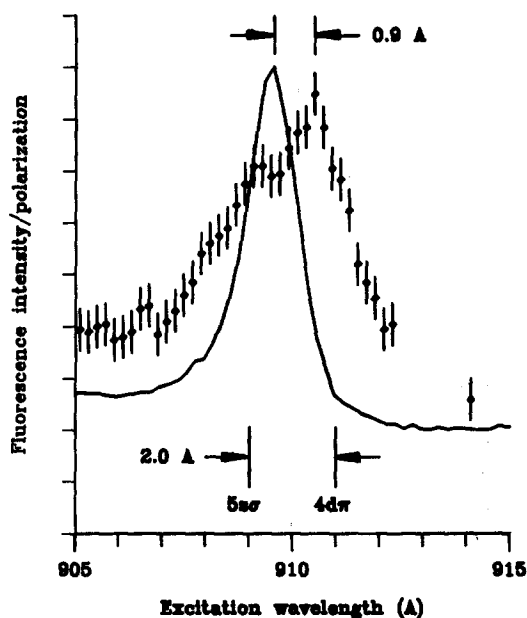


FIG. 4. Expanded view of fluorescence excitation (solid line) and fluorescence polarization (diamonds with error bars) spectra in region of the  $4d\pi$  and  $5s\sigma$  ( $\nu_R = 0$ ) resonances.

fraction itself vs wavelength, shifts between the excitation and polarization extrema can be verified accurately. All of the shifted features occur in the region of  $[ns\sigma, (n-1)d\pi]$  autoionization peaks. By way of contrast, the polarization peaks line up precisely with the excitation peaks for the  $nd\sigma$  series.

Finally, we note that the nonresonant (i.e., background) value of the fluorescence polarization can provide information on the relative strengths of the degenerate direct ionization channels.<sup>18</sup> In the region between the peaks, it appears that the fluorescence polarization dips to a minimum value  $P \sim -0.06$ , slightly higher than the analogous case of CO<sub>2</sub> photoionization.<sup>2</sup>

## IV. DISCUSSION

### A. Nonresonant polarization behavior

Figure 2 shows that the fluorescence polarization in nonresonant regions of the CS<sub>2</sub> spectrum is approximately  $P \sim -0.06$ , slightly more positive than the CO<sub>2</sub> case reported earlier, but still approaching a value of  $P = -1/13$ . This implies that the excitation transition dipole is perpendicular to the internuclear axis. Such behavior is expected if the  $\epsilon\sigma_g$  and  $\epsilon\delta_g$  continuum channels dominate at the expense of the  $\epsilon\pi_g$  continuum channel.<sup>2,18</sup> In other words, as the photoelectron is being ejected from a  $\pi_u$  orbital to form the  $A^2\Pi_u$  state nonresonantly, either the  $\epsilon\sigma_g$  or  $\epsilon\delta_g$  continuum channel dominates, resulting in a transition characterized by  $\Delta\lambda = \pm 1$ . To our knowledge, there have been no theoretical investigations of the nonresonant photoionization of CS<sub>2</sub>, but it is not surprising that its behavior would mimic that of CO<sub>2</sub>, where the  $\epsilon\delta_g$  channel dominates.<sup>2</sup> In fact, the nonresonant behavior of both CO<sub>2</sub> and CS<sub>2</sub> can be rationalized by examining the photoabsorption spectra at lower energy. Both absorption spectra reveal huge Rydberg resonances of

$\pi$  character, which could have the effect of depleting the  $\epsilon\pi_g$  continuum oscillator strength, resulting in a polarization index characterized by a perpendicular transition in the photon energy range presented in these fluorescence polarization studies.<sup>2</sup> It would be interesting to test this tentative explanation by computing the direct ionization cross sections for these channels.

There are a few possible explanations of why the measured polarization does not exactly equal the limiting value of  $P = -1/13$ . First, there could be some oscillator strength in the  $\epsilon\pi_g$  continuum channel. Second, spin-orbit coupling effects may reorient the absorption transition dipole in the molecular frame, analogous to the effect of hyperfine depolarization, described previously.<sup>22</sup> Also, collisions might result in the destruction of alignment, as the radiative lifetime of the CS<sub>2</sub><sup>+</sup> ( $A^2\Pi_u$ ) state is long,  $4.1 \pm 0.2 \mu\text{s}$ .<sup>23</sup> No pressure dependent measurements were performed, so the discrepancy between the observed and limiting polarization values might be due to collisional effects.

### B. Fluorescence polarization following resonant excitation

As in the previous CO<sub>2</sub> study,<sup>2</sup> it appears that most of the autoionizing features exhibit positive-going polarization profiles, although some do not. Figure 3 illustrates the utility of the method for symmetry labeling of autoionizing resonances, and the applicability of the simple mixing picture described previously.<sup>2</sup> The feature assigned as the  $4s\sigma$  resonance exhibits a polarization peak. Qualitatively, this is expected. The electronic transition populating the quasidecrete state is  $\sigma_u \rightarrow 4s\sigma$ , implying that the electronic transition dipole should be parallel to the internuclear axis, and that the fluorescence polarization (from the resonant contribution) should approach a limiting value of  $P = +1/7$ . By neglecting interference effects, it is straightforward to estimate the net fluorescence polarization, and this analysis will be discussed in the following section. First, though, we note that the behavior for the  $3d\pi$  feature is qualitatively different. Specifically, the polarization profile exhibits a local *minimum* at the resonance position. This is expected for  $\sigma_u \rightarrow 3d\pi$  excitation because the electronic transition moment for such a transition is perpendicular to the internuclear axis, resulting in a limiting value of  $P = -1/13$ . While the observed value is more positive than this limit, it is qualitatively in agreement with our expectation, as the wings of the  $4s\sigma$  autoionization profile extend over the  $3d\pi$  resonance. Thus it appears that the assignments of Ogawa and Chang<sup>3</sup> for these two resonances are correct, while some of the previous spectral assignments of these resonances were indeed in error. (See the discussion in Ref. 3.) Moreover, the polarization profiles for these two features stress the utility of the method for symmetry labeling.

Other facets of the excitation/polarization comparison are less straightforward, and one example is shown in Fig. 4. The  $5s\sigma$  resonance position does *not* correspond to the polarization maximum, as did the  $4s\sigma$  resonance. It is tempting to ascribe this misalignment to the fact that the  $5s\sigma$  and  $4d\pi$  resonances are not separated in the excitation spectrum, so the polarization maximum might be expected to be shifted

slightly to the “ $5s\sigma$  part” of the observed composite resonance. However, the observed polarization maximum is on the *high wavelength side* of the excitation peak, i.e., the “ $4d\pi$  part” of the excitation resonance, contrary to simple expectations. This unanticipated result lends itself to several explanations. First, the spectral assignments of Ogawa and Chang<sup>3</sup> for the higher- $n$  Rydberg features of the spectrum might be incorrect. This is unlikely given their strong spectroscopic evidence. A more likely explanation is that the simple mixing picture, in which it is assumed that the net polarization can be determined by simply obtaining a weighted average of the resonant and nonresonant contributions, is inadequate. While there is some validity to this procedure as evidenced by the fits to the CO<sub>2</sub> results<sup>2</sup> and much of the present data, it is clear that this simple mixing picture is, at best approximate, and must break down in some instances. For example, consider the case of an autoionizing window resonance, where the resonant weighting factor (the intensity *exceeding* the nonresonant contribution) is negative. In such a case, it is conceivable that the weighted average of polarizations would in fact exceed the physically meaningful limit  $P = -1$ . Thus, it is clear that interference terms must be included for a more general treatment. We expect that the observed misalignment is due to a breakdown of the simple mixing picture. A more clearcut limitation of the polarization averaging procedure is revealed by carrying out the same type of mixing analysis performed previously for the CO<sub>2</sub> case, as described below.

### C. Simulated polarization spectra

We simulate the CS<sub>2</sub> polarization spectrum in the region of the  $4d\sigma$  resonance using the procedure described previously.<sup>2</sup> This resonance is particularly suitable for this analysis, as the nonresonant background is rather flat in this vicinity and the resonance is broad and isolated. Thus the line shapes for the polarization and excitation spectra can be compared very accurately. The procedure is straightforward. The net polarization observed at any excitation wavelength is assumed to be the weighted average of resonant and nonresonant contributions. The averaging procedure is carried out in terms of the  $r$  index, defined as

$$r = (I_{\parallel} - I_{\perp}) / (I_{\parallel} + 2I_{\perp}) \quad (2)$$

The  $r$  index is related to the  $P$  index by

$$r = 2P / (3 - P) \quad (3)$$

and the weighted average  $r_{\text{net}}$  is obtained as follows:

$$r_{\text{net}} = (I_{\text{NR}} r_{\text{NR}} + I_{\text{R}} r_{\text{R}}) / (I_{\text{NR}} + I_{\text{R}}) \quad (4)$$

where  $I$  represents a dipole strength and the subscripts R and NR denote resonant and nonresonant, respectively. For the present case, we have estimated that  $r_{\text{NR}} = -0.04$  (corresponding to  $P = -0.06$ , as indicated by Fig. 2), and we assume that  $r_{\text{R}} = +0.10$  (i.e.,  $P = +1/7$ ). The weighting factors  $I_{\text{NR}}$  and  $I_{\text{R}}$  are obtained at every wavelength from the excitation spectrum as illustrated in the bottom frame of Fig. 5. The intensity below the horizontal solid line represents the nonresonant intensity and the intensity above is the resonant contribution. The simulated polarization spectrum

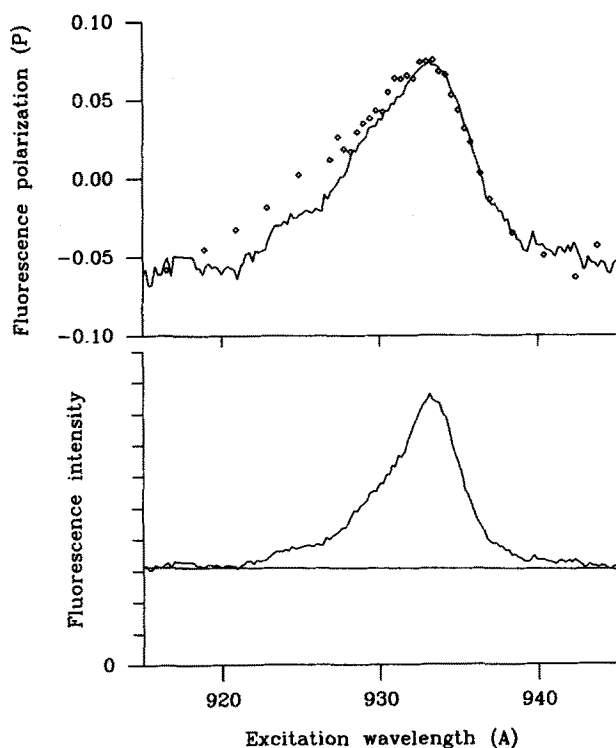


FIG. 5. Simulation of the polarization spectrum in the region of the  $4d\sigma$  resonance, obtained using the procedure outlined in the text. The bottom frame shows the fluorescence excitation spectrum, indicating the breakdown into resonant and nonresonant contributions. The top frame shows the measured polarization spectrum (diamonds), as well as the simulated polarization spectrum (solid line).

(following transformation back to the  $P$  index) is displayed in the top frame as the solid line, while the experimental points are shown as unconnected diamonds.

The qualitative agreement between the simulated curve and the experimental data is rather good. However, on the low wavelength side of the resonance the experimental values are consistently greater than the simulated values. It is not possible that a different spectral assignment would bring the simulated and experimental curves into agreement, as assigning the resonance as a  $\sigma \rightarrow \pi$  transition would make the simulated curve more negative, worsening the agreement. So, while the averaging procedure is adequate for assigning resonances and yields polarization line shapes qualitatively, it is inadequate for obtaining quantitative agreement. Clearly, interference effects must be considered as mentioned in the previous section, going beyond the mixing picture employed here.

There is another possible source of the observed discrepancy. It is possible that the exiting photoelectron exerts torque on the molecular frame, thereby altering the alignment and the subsequent fluorescence polarization.<sup>2</sup> Indeed, a recent study has shown that molecular rotation can be significantly affected by the photoelectron escape in the vicinity of an autoionization resonance.<sup>24</sup> If this is a source of the discrepancies noted in Fig. 5, significant dynamical information on molecular autoionization may be obtained by investigating polarization line shapes in greater detail. While theoretical treatments of ionic alignment following nonre-

sonant molecular photoionization have been extensive,<sup>18,22</sup> there is a complete lack of theoretical work for molecular autoionization, and these CS<sub>2</sub> results demonstrate that such efforts would be extremely useful.

There is also an instrumental extension that would be timely. Figure 5 shows that the region of largest deviation between the experimental data and the simulated curve is in the region of the  $\nu = 1$  component of the  $4d\sigma$  resonance. In order to emphasize the behavior in this region, it would be useful to stress this component at the expense of the  $\nu = 0$  component. If the fluorescence radiation were dispersed, the fluorescence originating from the  $\nu = 1$  level of the ion could be studied selectively, and it is likely that the profile for the  $\nu = 1$  level of the Rydberg level would be enhanced. Thus the present measurements provide a strong motivation for extending the method to include dispersed fluorescence. The key point is that autoionization, like most resonant excitation phenomena, frequently affects normally weak exit channels, so it is useful to probe individual vibrational channels selectively. Several dispersed fluorescence measurements have been performed recently<sup>15-17,24</sup> using synchrotron radiation excitation, and work is now in progress to extend these measurements to include polarization determinations.

## V. CONCLUSIONS

Fluorescence polarization measurements on CS<sub>2</sub><sup>+</sup> photoions have been carried out, corroborating the most recent spectral assignments of autoionizing Rydberg states in CS<sub>2</sub>. Two new aspects of such polarization experiments are revealed by these data. First, the polarization and excitation profiles are shifted in several instances. Second, the procedure employed in our previous study of CO<sub>2</sub>,<sup>2</sup> which utilized weighted averages of the resonant and nonresonant contributions, does *not* produce quantitative agreement with experiment. Further work is underway with vibrationally resolved measurements to extend and clarify these results.

## ACKNOWLEDGMENTS

This research was sponsored by the National Science Foundation (CHE-8310661), the Air Force Office of Scientific Research, Air Force Systems Command, USAF, under Grant No. AFOSR-84-0261, the U.S. Department of Energy, Office of Health and Environmental Research (Contract No. W-31-109-Eng-38), and the Office of Naval Research. GEL was the SURF (Synchrotron Ultraviolet Radiation Facility) Fellow at the National Bureau of Standards during a portion of this work.

<sup>1</sup>See, for example, J. L. Dehmer, D. Dill, and A. C. Parr, in *Photophysics and Photochemistry in the Vacuum Ultraviolet*, edited by S. McGlynn, G. Findley, and R. Huebner (Reidel, Dordrecht, 1985), p. 341, and references therein; also, I. Nenner and A. Beswick, in *Handbook on Synchrotron Radiation. Vol. II*, edited by G. V. Marr (North-Holland, Amsterdam, 1986).

<sup>2</sup>E. D. Poliakoff, J. L. Dehmer, A. C. Parr, and G. E. Leroy, *J. Chem. Phys.* **77**, 5243 (1982).

<sup>3</sup>M. Ogawa and H. C. Chang, *Can. J. Phys.* **48**, 2455 (1970).

<sup>4</sup>G. R. Cook and M. Ogawa, *J. Chem. Phys.* **51**, 2419 (1969).

<sup>5</sup>W. C. Price and D. M. Simpson, *Proc. R. Soc. London Ser. A* **165**, 272 (1938).

<sup>6</sup>Y. Tanaka, A. S. Jursa, and F. J. LeBlanc, *J. Chem. Phys.* **32**, 1205 (1960).

- <sup>7</sup>J. H. D. Eland and J. Berkowitz, *J. Chem. Phys.* **70**, 5151 (1979).
- <sup>8</sup>V. H. Dibeler and J. A. Walker, *J. Opt. Soc. Am.* **57**, 1007 (1967).
- <sup>9</sup>J. Momigny and J. Delwiche, *J. Chim. Phys. Phys. Chim. Biol.* **65**, 1213 (1968).
- <sup>10</sup>C. D. Caldwell and R. N. Zare, *Phys. Rev. A* **16**, 255 (1977); H. Klar, *J. Phys. B* **12**, L409 (1979); C. E. Theodosiu, A. F. Starace, B. R. Tambe, and S. T. Manson, *Phys. Rev. A* **24**, 301 (1981); C. H. Greene and R. N. Zare, *ibid.* **25**, 2031 (1982); W. Kronast, R. Huster, and W. Mehlhorn, *J. Phys. B* **17**, L51 (1984); H. Klar, *ibid.* **15**, 4535 (1982).
- <sup>11</sup>Z. H. Levine and P. Soven, *Phys. Rev. Lett.* **50**, 2074 (1983).
- <sup>12</sup>J. A. Stephens and D. Dill, *Phys. Rev. A* **31**, 1968 (1985).
- <sup>13</sup>D. Lynch, W. Huo, and V. McKoy (to be published).
- <sup>14</sup>M. Raoult, H. LeRouzo, G. Raseev, and H. Lefebvre-Brion, *J. Phys. B* **16**, 4601 (1983); P. Morin, I. Nenner, M. Y. Adam, M. J. Hubin-Franskin, J. Delwiche, H. Lefebvre-Brion, and A. Giusti-Suzor, *Chem. Phys. Lett.* **92**, 609 (1982).
- <sup>15</sup>E. D. Poliakoff, M.-H. Ho, G. E. Leroi, and M. G. White, *J. Chem. Phys.* **84**, 4779 (1986).
- <sup>16</sup>E. D. Poliakoff, M.-H. Ho, G. E. Leroi, and M. G. White, *J. Chem. Phys.* **85**, 5529 (1986).
- <sup>17</sup>E. D. Poliakoff, M.-H. Ho, M. G. White, and G. E. Leroi, *Chem. Phys. Lett.* **130**, 91 (1986).
- <sup>18</sup>E. D. Poliakoff, J. L. Dehmer, D. Dill, A. C. Parr, K. H. Jackson, and R. N. Zare, *Phys. Rev. Lett.* **46**, 907 (1981).
- <sup>19</sup>D. L. Ederer, B. E. Cole, and J. B. West, *Nucl. Instrum. Methods* **172**, 185 (1980).
- <sup>20</sup>L. C. Lee, D. L. Judge, and M. Ogawa, *Can. J. Phys.* **53**, 1861 (1975).
- <sup>21</sup>J. A. Coxon, P. J. Marcoux, and D. W. Setser, *Chem. Phys.* **17**, 403 (1976).
- <sup>22</sup>J. A. Guest, K. H. Jackson, and R. N. Zare, *Phys. Rev. A* **28**, 2217 (1983); J. A. Guest, M. A. O'Halloran, and R. N. Zare, *J. Chem. Phys.* **81**, 2689 (1984); C. H. Greene and R. N. Zare, *Annu. Rev. Phys. Chem.* **33**, 119 (1982); *Phys. Rev. A* **25**, 2031 (1982).
- <sup>23</sup>T. Ibuki and N. Sugita, *J. Chem. Phys.* **80**, 4625 (1984).
- <sup>24</sup>E. D. Poliakoff, J. C. K. Chan, and M. G. White, *J. Chem. Phys.* **85**, 6232 (1986).